

Band offsets at the crystalline/amorphous silicon interface from first-principles

K. Jarolimek,^{1,*} E. Hazrati,¹ R. A. de Groot,^{1,2} and G. A. de Wijs¹

¹*Radboud University, Institute for Molecules and Materials,
Heyendaalseweg 135, 6525 AJ Nijmegen, The Netherlands*

²*University of Groningen, Zernike Institute for Advanced Materials,
Nijenborgh 4, 9747 AG Groningen, The Netherlands*

(Dated: April 23, 2018)

The band offsets between crystalline and hydrogenated amorphous silicon (a-Si:H) are key parameters governing the charge transport in modern silicon heterojunction solar cells. They are an important input for macroscopic simulators that are used to further optimize the solar cell. Past experimental studies, using X-ray photoelectron spectroscopy (XPS) and capacitance-voltage measurements, have yielded conflicting results on the band offset. Here we present a computational study on the band offsets. It is based on atomistic models and density-functional theory (DFT). The amorphous part of the interface is obtained by relatively long DFT first-principles molecular-dynamics (MD) runs at an elevated temperature on 30 statistically independent samples. In order to obtain a realistic conduction band position the electronic structure of the interface is calculated with a hybrid functional. We find a slight asymmetry in the band offsets, where the offset in the valence band (0.30 eV) is larger than in the conduction band (0.17 eV). Our results are in agreement with the latest XPS measurements that report a valence band offset of 0.3 eV [M. Liebhaber *et al.*, Appl. Phys. Lett. **106**, 031601 (2015)].

PACS numbers: 73.21.Fg,71.23.Cq,71.15.Mb,71.15.Pd

I. INTRODUCTION

Silicon heterojunction (SHJ) solar cells combine the high-efficiency of c-Si wafer technology with the high-throughput and low-cost of hydrogenated amorphous silicon (a-Si:H) solar cells. The interface between crystalline and amorphous silicon lies at the heart of the SHJ solar cell. Since a-Si:H has a larger band gap than c-Si, band offsets are formed at the interface.

Experimentally the band offsets can be determined with techniques such as photoelectron spectroscopy and capacitance-voltage measurements. The reported values, however, scatter in a broad range.¹ This can be due to different deposition conditions of the a-Si:H layer or misinterpretation of the experimental results. On average it appears that the offset at the valence band is larger than at the conduction band (Ref. 1, p. 418).

Theoretical studies were mostly concerned with the atomic structure of the interface between c-Si and *pure* a-Si. Studies aimed either to obtain the interface energy (Ref. 2) or to study the velocity of the crystallization of a-Si on c-Si substrates.³ Some studies reported the electronic density of states, for the c-Si and a-Si:H parts of the interface, but did not comment on the band offsets.⁴⁻⁶ Santos *et al.*⁷ investigated defects present at the interface and the corresponding electronic levels within the band gap. George *et al.*⁷ modeled the electron spin resonance signal of defects at the interface. In terms of band offset calculations we are aware of two studies that obtained the values from the respective bulk materials.^{8,9} Peressi *et al.*,¹⁰ used a complete interface model, prepared with a combination of classical and first-principle molecular dynamics.¹⁰ Their amorphous part, was however, build from pure a-Si and often contained a high

defect concentration making the interface semi-metallic.

We present a calculation of band offsets that improves upon published studies in several aspects. The band offsets are calculated from an explicit interface model and not extracted from bulk properties only. There is a substantial (30) number of independent structural models that allows for reliable statistics. These models are prepared entirely from first-principles MD with defect levels sufficiently low to determine the band edges. The electronic structure is described with hybrid functionals that give a better description of band gaps and conduction band offsets.

This paper is organized as follows. Section II provides technical details on the calculations. The preparation of the structural models is described in Sec. III. In Sec. IV we discuss the electronic structure of the interface. Conclusions are presented in Sec. VI.

II. TECHNICAL DETAILS

Calculations were performed on the level of density functional theory (DFT) with the Vienna Ab initio Simulation Package (VASP).^{11,12} Electron-ion interactions were described using the projector augmented wave (PAW) method.^{13,14}

We performed molecular dynamics calculations with the Verlet algorithm. The canonical NVT ensemble was simulated using the algorithm by Nosé.¹⁵ We increased the mass of hydrogen to 10 amu, which allowed us to use a slightly longer time step of 1.5 fs. During the whole MD run and the relaxation, we used the Γ point for Brillouin zone sampling. The kinetic energy cut-off was set relatively low at 150 eV. This was made possible by us-

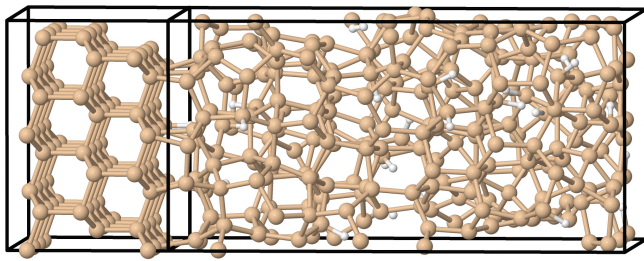


FIG. 1: (Color online) One of the simulation cells used in the present study. The crystalline cell was terminated with two distinct (111) surfaces. Si and H atoms are drawn as brown and white spheres, respectively.

ing PAW potentials with larger core radii.¹⁶ For Si the s -, p - and d -partial wave radii were 2.2, 2.7 and 2.7 a.u., respectively. For H both s - and p -partial wave radii were 1.3 a.u. The performance of the potentials was tested on bulk c -Si and the SiH_4 molecule. The equilibrium Si-Si and Si-H bond lengths decreased by less than 0.01 Å, when using the less accurate potentials. The frequency of the TO mode in c -Si decreased by 1 %, while the frequency of the Si-H stretching mode in SiH_4 was lower by 5 %. The above described tests, as well as all dynamic calculations were performed with the generalized gradient approximation (GGA) using the PBEsol functional.¹⁷

Although the GGA gives accurate structural properties it is known to underestimate band gaps. In order to obtain realistic band gaps and offsets,¹⁸ all static calculations were performed with a hybrid functional. This type of functional include a part of exact exchange from Hartree-Fock theory. We used the HSE06 hybrid functional^{19,20} with a screening parameter of 0.2 Å⁻¹. PBE potentials with a 250 eV cut-off were used. The Brillouin zone was sampled with a Γ centered $2 \times 2 \times 1$ mesh, while the Hartree-Fock kernel was evaluated only at Γ . The density of states was calculated with a Gaussian smearing with a width of 0.05 eV.

III. PREPARATION OF THE STRUCTURE

In order to simulate the interface we constructed a total of 30 simulation cells with dimensions of $15.35 \times 13.30 \times 36.00$ Å³. Periodic boundary conditions were applied in all three dimensions. The cells were divided into a crystalline and an amorphous part. The crystalline part consisted of 3 double layers of Si atoms, centered within a 9.40 Å wide region (see Fig. 1).

The amorphous part contains 256 Si atoms and 30 H atoms, which leads to a H concentration of 10.5 at. % and mass density of 2.21 g/cm³. These values are representative of device-quality bulk a -Si:H.²¹ Initially the atoms were placed randomly in the cell, followed by an annealing step at 1100 K for 135 ps, using DFT molecular-dynamics. The optimum annealing temperature was determined by a series of tests on bulk a -Si:H cells. Low

temperatures did not result in sufficient movement of atoms and the system could be trapped in a high-energy local minimum. On the other hand, a too high temperature could result in a liquid-like structure with many over-coordinated defects.

After the annealing step a relaxation was performed that brought the system to the nearest local energy minimum. During the annealing and relaxation, atoms in the crystalline part were fixed and were not allowed to move. As a last step we doubled the amount of c -Si in the simulation cell. The cell vector perpendicular to the interface increased from 36.00 to 45.40 Å.

In the following we analyze the structure of the middle portion of the amorphous cell. Only atoms that were located more than 3.1 Å from the nearest interface were considered. The mean Si-Si and Si-H bond lengths were 2.37 and 1.53 Å, respectively. These values compare well with diffraction measurements on bulk a -Si:H, that give 2.35 and 1.48 Å, respectively.²² On average we found 2.1 H-H bonds (H_2 molecules) per simulation cell. A more sensitive measure of strain in the amorphous network is the bond angle distribution. To proceed, we define the following cut-off distances: $r_{\text{Si-Si}} = 2.76$ Å and $r_{\text{Si-H}} = 1.79$ Å. The bond angles were calculated only between Si-Si bonds and Si-H bonds were ignored. We obtained an average value of 108.9°, that is close to the bulk experimental value of 109.5°. ²² The bond angle RMS deviation can be inferred from the width of the TO peak, as measured by Raman spectroscopy. The experimental values of 8.7° (Ref. 23) and 9.3° (Ref. 24) are a bit smaller than the calculated value of 12.6°. This points to some additional strain in our models, although one has to keep in mind that the experiments were done on bulk a -Si:H. It is reasonable to assume that the amorphous network is more strained close to the interface with c -Si.

Another important property of the a -Si:H model is the number of coordination defects. We find that the number of 5-fold coordinated Si atoms is higher than the number 3-fold coordinated ones (4.6 and 1.4 atoms per simulation cell, respectively). Tosolini *et al.*⁶ reported an opposite trend and Santos *et al.*²⁵ found 3-fold coordinated atoms but did not report on the 5-fold coordinated ones. We also find H atoms in a bridging position (0.2 atoms per simulation cell). Santos *et al.*²⁵ also investigated this defect but it was not reported by Tosolini *et al.*⁶ The number of other defects is less than 0.1 per simulation cell. The differences with Santos *et al.* and Tosolini *et al.* are possibly due to the different method used to prepare the structure: they used tight-binding MD whereas we used DFT MD. The presence of the interface might lead to more 5-fold coordinated Si atoms. In our previous DFT MD study on pure a -Si:H, which had similar H concentration, we obtained comparable numbers of 3-fold and 5-fold coordinated Si atoms.²⁶

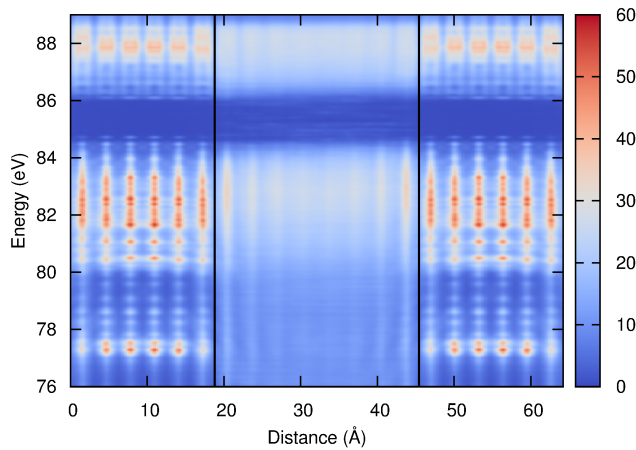


FIG. 2: (Color online) Position-resolved DOS (in $10^{21} \text{ cm}^{-3} \text{ eV}^{-1}$, HSE06) along the normal of the interface and obtained as an average over 30 cells. The crystalline part of the cell is shown twice in order to see both interfaces more clearly. Interfaces are marked by vertical lines. The zero of energy is the mean potential at the Si atom cores in the central part of the crystalline region.

IV. ELECTRONIC STRUCTURE OF THE INTERFACE

Because we had to average over 30 simulation cells we needed to align the single-particle energy levels in the different cells. We used the mean potential at core of the Si atoms in the mid-section of the crystalline part (2 layers, 32 atoms) for this purpose. The potential at a particular atomic site was calculated with a unit test charge that has a radius of 0.989 Å.

In Fig. 2 we show position-resolved density of states of the interface. There is a marked difference between the crystalline and amorphous part of the interface. In the crystalline part the 6 double layers of Si atoms can be easily identified as areas with high density of states. The disorder in the amorphous part leads to a smeared out DOS. Some ordering is visible close to the crystalline part. Evidently the “memory” of the layered structure is lost only gradually when moving away from the fixed crystalline part. The band gap is centered at around 85 eV and has a dark blue color.

In the following we consider the DOS of the middle section of the amorphous part that is representative of bulk a-Si:H (see Fig. 3). We discard 3.1 Å (width of one double layer) from both edges of the amorphous part. The determination of a band gap for amorphous semiconductors is somewhat ambiguous.²⁷ We used the definition by Tauc, which is the simplest one. In this model the valence and conduction band DOS follow a square root dependence on energy (see red lines in Fig. 3). It is clear that the model is valid only for the middle range of DOS values. We chose an interval that spans from 30 to 80 % of the maximum DOS value (at $28 \times 10^{21} \text{ cm}^{-3} \text{ eV}^{-1}$). This allowed us to find the energy ranges to fit the Tauc model

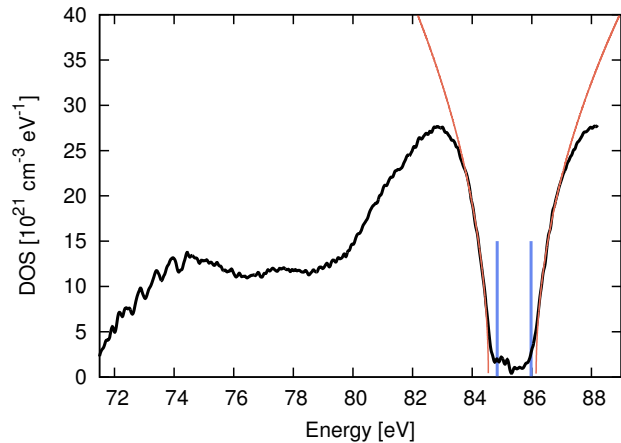


FIG. 3: (Color online) HSE06 DOS of the amorphous part of the interface (black lines). Tauc fit to the DOS is shown in red. Position of band edges of c-Si are marked with blue vertical lines. The zero of energy is the mean potential at the Si atom cores in the central part of the crystalline region.

to the calculated DOS. Using a lower limit of 30 % effectively means that we rely on the extended states to define the position of the band edge and that we suppress the effect of tail and defect states. This should also minimize the effect of stress in the structural models. After performing a least square fit we obtained a band gap of 1.60 eV (HSE06), which is quite close to the experimental Tauc gap of 1.7 eV.²⁸ We tested the sensitivity of the obtained band edges on the number of cells used in the averaging. When using the first 10 or 20 cells the position of the band edges changed by less than 0.01 eV. Band offsets were affected by the same amount.

As a next step we needed to obtain the position of the c-Si band edges. One might assume that one can do this by calculating the DOS of the crystalline part of the interface, in an analogous way as was done for the amorphous part. It turned out, however, that the band gap obtained in this way is overestimated. We argue that this is due to quantum confinement effects. To illustrate this we selected one of the cells and calculated its band structure with the GGA functional (see Fig. 4). We chose a path in reciprocal space that is the same as for a primitive c-Si cell with 2 atoms.³² The band structure of the interface cell is color coded so that we can identify states (in red) that are localized in the crystalline part of the interface. We observe that the valence band maximum is still at Γ and the conduction band minimum is close to the X point. In both cases the bands are less dispersive than in bulk c-Si. The (PBEsol) band gap is larger (0.69 eV) compared to bulk c-Si (0.46 eV). When we removed 3 double layers of Si atoms (9.40 Å) from the crystalline part, we obtained an even larger band gap of 0.96 eV. Conversely adding 3 double layers decreased the band gap to 0.58 eV. We note that we expect only weak quantum confinement and charge localization effects in the amorphous part, since the charge carriers in bulk a-Si:H

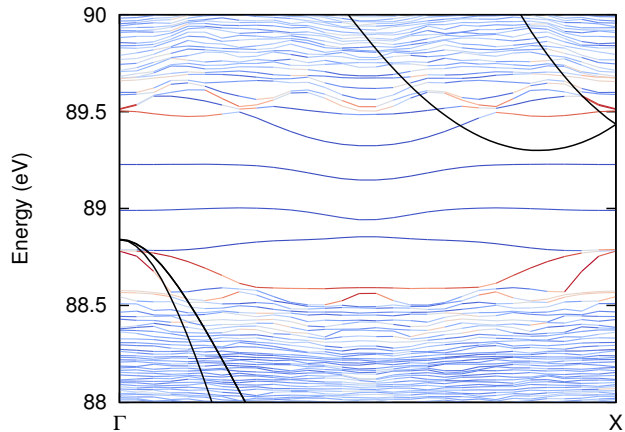


FIG. 4: (Color online) PBEsol Band structure of the c-Si/a-Si:H interface (blue/red lines) compared to bulk c-Si (black lines). States marked with red color (light grey) are localized in the crystalline part of the interface. The zero of energy is the mean potential at the Si atom cores in the central part of the crystalline region.

are localized to begin with.²⁹

In order to circumvent the problem with quantum confinement in the c-Si part we followed a different approach. We calculated the band structure of c-Si with 2 atoms in the unit cell and obtained a band gap of 1.14 eV (HSE06). The position of the top of the valence band (at Γ) and bottom of conduction band (between Γ and X) were again referenced to the potential at core of the Si atoms. These values were then combined with the DOS of a-Si:H (see blue lines in Fig. 3). The band offsets were calculated as differences between the positions of the band edges in c-Si and a-Si:H. For the valence and conduction offset we obtained 0.30 and 0.17 eV, respectively.

V. DISCUSSION

Our calculated valence band offset (0.30 eV) is in good agreement with the latest X-ray photoelectron spectroscopy (XPS) measurement of 0.3 eV.³⁰ Kleider performed a careful analysis of capacitance-voltage measurements (C-V) and reports a valence and conduction offset of 0.40 and 0.15 eV, respectively (Ref. 1, p. 405). Both are close to our values (0.30 and 0.17 eV). Kleider notes that some of the previous studies did not take into account the specific properties of a-Si:H in their analysis. This could then explain the large spread in the reported values.

Previous theoretical studies used models of bulk c-Si and a-Si:H to calculate band offsets. Our results for the valence offset fall in-between the reported values. Allan *et al.* used a ~ 4000 atom model of a-Si:H and in the tight-binding approximation obtained a valence offset of 0.36 eV. The H concentration was 8 at. %, close to our value, but the mass density was not reported.

It is likely that the final value is, however, larger since the band edge states used are somewhat localized (band tails). This is corroborated by the fact that the reported band gap of a-Si:H is too small (1.36 eV).⁸ Van de Walle used the so called “model-solid” theory to obtain a valence band offset of 0.2 eV.⁹ Van de Walle also derived relations between the offsets and a-Si:H density and H concentration. The a-Si:H model has a similar H concentration (11 at. %) as our models, but the density is higher (set to c-Si value). When we substitute our density, to make a more fair comparison, the valence offset reduces to 0.07 eV. It is difficult to pinpoint the origin of the discrepancies between our results and the older studies. The fact that the interface was not considered directly might play a role, together with differences in a-Si:H structure preparation and density. In our view the most likely explanation is that the methods to locate the band edges in a-Si:H were different. When small cells or a small number of cells is used, it is difficult to distinguish between extended and tail states.

In terms of SHJ solar cell performance there seems to be an optimum value for the valence band offset. Several studies simulated the performance of n-type wafer based SHJ cells by solving the Poisson and charge carrier continuity equations (see Ref. 31 and references therein). The studies agree that a valence offset larger than 0.5 eV leads to a sharp decrease in solar cell efficiency. This is caused by accumulation and subsequent recombination of holes on the c-Si side of the c-Si/a-Si:H interface. Shen *et al.* put the optimum offset at 0.45 eV.³¹

VI. CONCLUSIONS

We have prepared an atomistic model of the crystalline/amorphous silicon interface. The amorphous part is hydrogenated and is thus relevant for technological applications such as silicon heterojunction solar cells. In order to obtain reliable results we averaged the calculated quantities over 30 statistically independent simulation cell. Atomic models were prepared with molecular-dynamics, where forces are computed with density functional theory. This should give an accurate description of the interface region that contains a large number of strained bonds.

The electronic structures of the particular simulation cells are aligned at the mean potential at the Si atom cores in the crystalline part of the interface. We have attempted to extract the band offsets directly from the position resolved density of states. This was possible in the amorphous part but not in the crystalline part of the interface due to quantum confinement effects. To resolve this issue we used band edges from a bulk c-Si calculation and performed again an alignment at the core potential of Si atoms. We obtain a valence and conduction band offset of 0.30 and 0.17 eV. This is in good agreement with recent XPS and C-V measurements.^{1,30}

Acknowledgments

We thank Prof. Kresse for the special, extra-soft PAW data sets. This work was supported by Technology Foundation STW within the framework of the FLASH perspective program. We thank SURFsara

(www.surfsara.nl) for the support in using the Lisa Compute Cluster. The work of RAG is part of the research program of the Foundation for Fundamental Research on Matter (FOM). Both SURFsara and FOM are financially supported by the Netherlands Organization for Scientific Research (NWO).

-
- * Present address: University of Kentucky, Center for Applied Energy Research, 2540 Research Park Drive, Lexington, KY 40511, USA
- ¹ J.-P. Kleider, in *Physics and Technology of Amorphous-Crystalline Heterostructure Silicon Solar Cells*, edited by W. G. J. H. M. van Sark, L. Korte, and F. Roca (Springer, Berlin, 2012).
 - ² S. Izumi, S. Hara, T. Kumagai, and S. Sakai, *Comp. Mater. Sci.* **31**, 279 (2004).
 - ³ C. Krzeminski, Q. Brulin, V. Cuny, E. Lecat, E. Lampin, and F. Cleri, *J. Appl. Phys.* **101**, 123506 (2007).
 - ⁴ M. Nolan, M. Legesse, and G. Fagas, *Phys. Chem. Chem. Phys.* **14**, 15173 (2012).
 - ⁵ B. C. Pan and R. Biswas, *J. Appl. Phys.* **96**, 6247 (2004).
 - ⁶ M. Tosolini, L. Colombo, and M. Peressi, *Phys. Rev. B* **69**, 075301 (2004).
 - ⁷ B. M. George, J. Behrends, A. Schnegg, T. F. Schulze, M. Fehr, L. Korte, B. Rech, K. Lips, M. Rohrmüller, E. Rauls, et al., *Phys. Rev. Lett.* **110**, 136803 (2013).
 - ⁸ G. Allan, C. Delerue, and M. Lannoo, *Phys. Rev. B* **57**, 6933 (1998).
 - ⁹ C. G. Van de Walle and L. H. Yang, *J. Vac. Sci. Technol. B* **13**, 1635 (1995).
 - ¹⁰ M. Peressi, L. Colombo, and S. de Gironcoli, *Phys. Rev. B* **64**, 193303 (2001).
 - ¹¹ G. Kresse and J. Hafner, *Phys. Rev. B* **47**, 558 (1993).
 - ¹² G. Kresse and J. Furthmüller, *Phys. Rev. B* **54**, 11169 (1996).
 - ¹³ P. E. Blöchl, *Phys. Rev. B* **50**, 17953 (1994).
 - ¹⁴ G. Kresse and D. Joubert, *Phys. Rev. B* **59**, 1758 (1999).
 - ¹⁵ S. Nosé, *J. Chem. Phys.* **81**, 511 (1984).
 - ¹⁶ L. E. Hintzsche, C. M. Fang, T. Watts, M. Marsman, G. Jordan, M. W. P. E. Lamers, A. W. Weeber, and G. Kresse, *Phys. Rev. B* **86**, 235204 (2012).
 - ¹⁷ J. P. Perdew, A. Ruzsinszky, G. I. Csonka, O. A. Vydrov, G. E. Scuseria, L. A. Constantin, X. Zhou, and K. Burke, *Phys. Rev. Lett.* **100**, 136406 (2008).
 - ¹⁸ J. Heyd, J. E. Peralta, G. E. Scuseria, and R. L. Martin, *J. Chem. Phys.* **123**, 174101 (2005).
 - ¹⁹ J. Heyd, G. E. Scuseria, and M. Ernzerhof, *J. Chem. Phys.* **118**, 8207 (2003).
 - ²⁰ J. Heyd, G. E. Scuseria, and M. Ernzerhof, *J. Chem. Phys.* **124**, 219906 (2006).
 - ²¹ Z. Remeš, M. Vaněček, P. Torres, U. Kroll, A. H. Mahan, and R. S. Crandall, *J. Non-Cryst. Solids* **227**, 876 (1998).
 - ²² R. Bellissent, A. Menelle, W. S. Howells, A. C. Wright, T. M. Brunier, R. N. Sinclair, and F. Jansen, *Physica B* **156**, 217 (1989).
 - ²³ S. Vignoli, P. Mélinon, B. Masenelli, P. R. i Cabarrocas, A. M. Flank, and C. Longeaud, *J. Phys.: Condens. Matter* **17**, 1279 (2005).
 - ²⁴ M. Wakagi, K. Ogata, and A. Nakano, *Phys. Rev. B* **50**, 10666 (1994).
 - ²⁵ I. Santos, M. Cazzaniga, G. Onida, and L. Colombo, *J. Phys.: Condens. Matter* **26**, 095001 (2014).
 - ²⁶ K. Jarolimek, R. de Groot, G. A. de Wijs, and M. Zeman, *Phys. Rev. B* **79**, 155206 (2009).
 - ²⁷ S. K. O'Leary, *J. Mater. Sci.: Mater. Electron.* **15**, 401 (2004).
 - ²⁸ R. A. Street, *Hydrogenated amorphous silicon* (Cambridge University Press, Cambridge, 1991).
 - ²⁹ K. Jarolimek, R. A. de Groot, G. A. de Wijs, and M. Zeman, *Phys. Rev. B* **90**, 125430 (2014).
 - ³⁰ M. Liebhaber, M. Mews, T. F. Schulze, L. Korte, B. Rech, and K. Lips, *Appl. Phys. Lett.* **106**, 031601 (2015).
 - ³¹ L. Shen, F. Meng, and Z. Liu, *Solar Energy* **97**, 168 (2013).
 - ³² The primitive cell was cut from the interface cell and thus the $\langle 111 \rangle$ vector points along the interface normal and along the z -axis. This allows us to use the same Cartesian coordinates (0.1303, 0.0752, 0.1064) \AA^{-1} for the X point, in both band structure calculations.